

Inherent stochasticity precludes hysteresis in gene regulatory networks

Manuel Pájaro¹, Irene Otero-Muras¹, Carlos Vázquez², and Antonio A. Alonso^{*1}

¹Process Engineering Group, IIM-CSIC. Spanish Council for Scientific Research.
Eduardo Cabello 6, 36208 Vigo, Spain

²Department of Mathematics, University of A Coruña. Campus Elviña s/n, 15071 A
Coruña, Spain

October 25, 2018

1 Abstract

Cell fate determination, the process through which cells commit to differentiated states, has been shown to be mediated by gene regulatory motifs with mutually exclusive expression states. The classical picture for deterministic cell decision making includes bistability and hysteresis. Despite numerous experimental works supporting evidence of hysteresis in gene regulatory networks, such phenomenon may not be compatible with the stochasticity underlying gene regulation dynamics. Here we show how under sufficiently slow dynamics, the dependency of the transient solutions on the initial state of the cells can be mistakenly interpreted as hysteresis and, to quantify this phenomenon, we provide an estimate of the convergence rate to the equilibrium. We also introduce the equation of a natural landscape capturing the evolution of the system that, unlike traditional cell fate potential landscapes, is compatible with the notion of coexistence at the microscopic level.

2 Introduction

In a deterministic description, binary decision making is attributed to the irreversible state transition between two mutually exclusive stable steady states in response to a signal. This state transition is usually governed by regulatory motifs with the capacity for bistability and

*Author to whom correspondence should be addressed. E-mail: antonio@iim.csic.es

hysteresis [1], ensuring that the system does not switch back immediately when the signal is removed [2].

The stochastic dynamic behaviour of a gene regulatory network is described by a Chemical Master Equation (CME), which gives the time evolution of the probability distribution of the system state. The stationary solution of the CME is unique, not depending on the initial state of the system [3] and therefore intrinsic molecular noise inherent to gene regulatory processes is incompatible with memory effects or hysteresis. However, in numerous studies hysteresis has been found in gene regulatory networks with significant levels of stochasticity [4, 5, 6, 7].

In the context of phenotypic switching and cell fate determination, three different scenarios have been distinguished and experimentally observed for binary decision making: deterministic *irreversible* [8, 9, 10], stochastic *reversible* [11] and stochastic yet *irreversible* state transitioning [12]. Reversibility is understood here as the capacity of individual cells to switch back in absence of external signals. According to a pseudo-potential interpretation, dynamics are directed by a pseudo-potential landscape divided by a separatrix into two basins of attraction such that each local minimum correspond to a specific cellular state. Stochastic irreversible transitions are found to appear when cells are initialized on or near the separatrix [12].

In this letter, we show that for stochastic gene regulatory networks hysteresis and apparent irreversibility at the single cell level are transient effects, and disappear at the stationary state. Since the stationary solution of the CME is unique [3], if the solution corresponds to a bimodal distribution, state transitions at the single cells level occur necessarily in a random and spontaneous manner, switching back and forth between attractors.

In [13] an energy potential landscape as the negative logarithm of the probability distribution is determined experimentally, as well as the transition rates, based on previous theoretical studies (e. g. [14]). Here we provide a theoretical basis that explains coexistence of different expression states, and predict the potential landscape via Master Equation [15, 16] together with time constants of the system. Here, the Chemical Master Equation is accurately approximated under the assumption of protein bursting [15]. A clear link between the characteristic kinetic parameters of regulation dynamics and the resulting dynamic behaviour is established.

3 Results

We consider the simplest gene regulatory motif exhibiting hysteresis, a single gene with positive self-regulation. In a deterministic description, the evolution of the amounts of *mRNA* and

protein X (m and x , respectively) for the system in Fig. 1 is given by a set of ODEs:

$$\begin{aligned}\frac{dm}{dt} &= k_m c(x) - \gamma_m m \\ \frac{dx}{dt} &= k_x m - \gamma_x x\end{aligned}\tag{1}$$

where $k_m c(x)$ is the transcription rate, essentially proportional to the input function $c(x)$ which collects the expression from the activated and inactivated promoter states. This function incorporates the effect of protein self-regulation and takes the form [17, 18]:

$$c(x) = (1 - \rho(x)) + \rho(x)\varepsilon,\tag{2}$$

with $\rho(x)$ being a Hill function [19] that describes the ratio of promoter in the inactive form as a function of bound protein:

$$\rho(x) = \frac{x^H}{x^H + K^H},\tag{3}$$

this can be interpreted as the probability of the promoter being in its inactive state, where $K = \frac{k_{\text{off}}}{k_{\text{on}}}$ is the equilibrium binding constant and $H \in \mathbb{Z} \setminus \{0\}$ is an integer (Hill coefficient) which indicates whether protein X inhibits ($H > 0$) or activates ($H < 0$) expression. Finally, expression (2) includes basal transcription or leakage with a constant rate $\varepsilon := \frac{k_\varepsilon}{k_m}$ (see Fig.1) typically much smaller than 1.

Assuming that $mRNA$ degrades faster than protein X we have that $m^* = k_m c(x)/\gamma_m$ and model (1) reduces to:

$$\frac{dx}{d\tau} = -x + abc(x),\tag{4}$$

where $\tau = t\gamma_x$, $a = k_m/\gamma_x$ and $b = k_x/\gamma_m$.

Fig. 2 shows the equilibrium of the system as the critical parameter b is varied. For b values below a given threshold, there is a unique stable steady state of low protein x towards which the system evolves independently of the initial conditions. For input signals above a second threshold, the system evolves towards a unique stable steady state of high x . For signal values within both thresholds, the system is bistable, and evolves towards one stable state or another depending on the initial conditions. This system has *memory*, since steady state values provide information about the system's past. In systems with hysteresis (dependency of the state of the system on its past), forward and reverse induction experiments follow different paths resulting in a hysteresis loop (the system switches back and forth for different values of the control parameter), as shown in the figure.

Gene expression is inherently stochastic. Next, we approximate the solution of the CME describing the stochastic dynamics of the system under study. Assuming that $mRNA$ degrades faster than protein X , as it is the case in most prokaryotic and eukaryote organisms [20], protein can be assumed to be produced in bursts [21, 22, 17, 18] at a frequency $a = \frac{k_m}{\gamma_x}$, where

k_m is the transcription rate and γ_x is the rate of protein degradation. From this assumption, it follows [22, 18] that the temporal evolution of the associated probability density function $p : \mathbb{R}_+ \times \mathbb{R}_+ \rightarrow \mathbb{R}_+$ can be described by a Partial Integro-Differential Equation (PIDE) of the form:

$$\frac{\partial p(\tau, x)}{\partial \tau} - \frac{\partial [xp(\tau, x)]}{\partial x} = a \int_0^x \omega(x-y)c(y)p(\tau, y) dy - ac(x)p(\tau, x), \quad (5)$$

where x and τ correspond with the amount of proteins and dimensionless time, respectively. The later variable is associated to the time scale of the protein degradation and can be expressed as $\tau = \gamma_x t$. In addition, $\omega(x-y)$ is the conditional probability for protein level to jump from a state y to a state x after a burst, which is proportional to:

$$\omega(x-y) = \frac{1}{b} \exp\left[\frac{-(x-y)}{b}\right], \quad (6)$$

with $b = \frac{k_x}{\gamma_m}$ representing the burst size. The stationary form of the one dimensional equation (5) has the following analytical solution [17, 18]:

$$p^*(x) = C [\rho(x)]^{\frac{\alpha(1-\varepsilon)}{H}} x^{-(1-a\varepsilon)} e^{-\frac{x}{b}}, \quad (7)$$

where $\rho(x)$ is defined in (3) and C is a normalizing constant such that $\int_0^\infty p^*(x) dx = 1$. It is known that the equilibrium solution associated to a CME is unique and therefore stable [3]. This is also the case for the Friedman equation (5) whose stability has been recently proved by entropy methods [23, 24], which eventually makes it to qualify as a master equation itself. Here we use a one dimensional case for simplicity, it is important to remark that stability properties remain valid for higher dimensions (multiple gene and proteins).

In Fig. 3 we depict the mean x -value of transient and stationary solutions as a function of the b parameter for two different initial conditions. It can be observed that, while the mean x -values of the stationary solution do not depend on the initial conditions, the means obtained at the transients depend on the initial number of proteins.

Note that under sufficiently slow dynamics, transient values may look stationary, thus leading to plots (red and blue lines) that resemble hysteresis, as different mean values coexist within a given interval of the b parameter. Interestingly, this interval coincides with bimodal distributions in which the two most probable states are separated by a region, in the protein space, with very low probability. This explains recent experimental observations [7] in which the range of apparent hysteresis was found to shrink with time.

Fig. 4 compares transient and stationary distributions for different values of the b parameter and different initial conditions. In fact, the low probability region acts as a barrier that hinders transitions between low and high protein expression and in this way contributes to slow down the dynamics towards the corresponding stationary distribution.

In order to compute an estimate of the convergence rate to equilibrium we make use of entropy methods [24, 23] defining the entropy norm:

$$G = \int_0^\infty H(u(\tau, x))p^*(x)dx \quad (8)$$

where $H(u(\tau, x))$ is a convex function in u , that in this study has been chosen to be $H(u) = u^2 - 1$, with $u = p(\tau, x)/p^*(x)$. According to [23, 24], G obeys the following differential inequality:

$$\frac{dG}{dt} \leq -\eta G, \quad (9)$$

with η being a positive constant somehow related to regulation (parameters H and K), as well as the transcription-translation kinetics (a , b). The smaller η , the slower its convergence towards the corresponding equilibrium solution. Computing η requires a full simulation of (5) with SELANSI [16] up to reach the equilibrium distribution for each parameter on a given range, what is computationally involved. In Fig. 6 we compare the convergence rates η for two different initial conditions and different values of b , showing that the smaller η values correspond to the solution near equilibrium which lies within the hysteresis region in the b parameter space.

To avoid simulation burden, we propose a truncation method to compute the rates of convergence using the discrete jump process representation, precursor of Friedman PIDE model, by making the protein amount a continuous variable [15]. The discrete process is depicted in Fig. 5 and truncated to an N total number of proteins.

Let $\mathcal{P} : \mathbb{R}_+ \times \mathbb{N} \rightarrow [0, 1]$, be the probability of having n proteins at time t . The time evolution of $\mathcal{P}(t, n)$ is given by the following CME with jumps, that reads:

$$\frac{d\mathcal{P}(t, n)}{dt} = \sum_{i=0}^{n-1} g_i^n \mathcal{P}(t, i) - \sum_{i=n+1}^{\infty} g_n^i \mathcal{P}(t, n) + \gamma_x(n+1)\mathcal{P}(t, n+1) - \gamma_x(n)\mathcal{P}(t, n), \quad (10)$$

where the transition probability g_i^j is proportional to the production rate of messenger RNA, so that:

$$g_i^j := \frac{a}{b} c(i) e^{\frac{i-j}{b}}, \quad \forall j > i. \quad (11)$$

In order to obtain an approximation of the convergence rate of the PIDE model (5) towards the stationary state, we use the truncated form of the discrete equation (10). Let be N the maximum possible number of proteins. Then, equation (10) can be written in matrix form as:

$$\frac{d\mathcal{P}(t, n)}{dt} = \mathcal{M}\mathcal{P}(t, n), \quad (12)$$

where the matrix \mathcal{M} reads:

$$\mathcal{M} = \begin{pmatrix} -d_0 & 1\gamma_x & 0 & \cdots & 0 & 0 & 0 \\ g_0^1 & -d_1 & 2\gamma_x & \cdots & 0 & 0 & 0 \\ g_0^2 & g_1^2 & -d_2 & \ddots & 0 & 0 & 0 \\ \vdots & \vdots & & \ddots & \ddots & & \vdots \\ g_0^{N-2} & g_1^{N-2} & g_2^{N-2} & \cdots & -d_{N-2} & (N-1)\gamma_x & 0 \\ g_0^{N-1} & g_1^{N-1} & g_2^{N-1} & \cdots & g_{N-2}^{N-1} & -d_{N-1} & N\gamma_x \\ g_0^N & g_1^N & g_2^N & \cdots & g_{N-2}^N & g_{N-1}^N & -d_N \end{pmatrix}. \quad (13)$$

with the elements of the diagonal d_i being of the form:

$$d_i = \begin{cases} i\gamma_x + \sum_{n=i+1}^N g_i^n & \text{if } i = 0, \dots, N-1, \\ N\gamma_x & \text{if } i = N, \end{cases} \quad (14)$$

equivalently:

$$d_i = i\gamma_x + \frac{ac(i)}{b\left(e^{\frac{1}{b}} - 1\right)} \left(1 - e^{\frac{i-N}{b}}\right) \quad \text{for } i = 0, \dots, N. \quad (15)$$

The steady state is given by the null space of matrix \mathcal{M} , i.e. the normalized eigenvector associated to the zero eigenvalue. Since the graph associated to matrix \mathcal{M} (Fig. 5) has one trap, all the eigenvalues are negative except one (which is zero) [25].

Fig. 7 compares the highest negative eigenvalue of matrix \mathcal{M} (13) with the convergence rate η obtained by simulation, for different values of the parameter b . In the parameter range where bimodal distributions coexist, the highest negative eigenvalue λ_1 is a good approximation of the convergence rate of the PIDE model.

Remarkably, low convergence rates coincide with the parameter region in which bimodal behaviour occurs. This supports the fact that experimental distributions may be likely to be mistaken as stationary, what in turns can be wrongly interpreted as a hysteresis phenomenon.

This proof of concept has served to illustrate how hysteresis, as it is known in deterministic nonlinear systems, has not an equivalence in a microscopic world governed by a CME. In fact, diagrams suggesting hysteresis-like behaviour were obtained under transients that resemble stationary solutions due to the extremely slow dynamics at which bimodal distributions evolve. Nonetheless, some correspondence can be drawn between the most frequently visited states on a microscopic system and the stable states on the deterministic counterpart. As it has been discussed in [18], the extremes states of a stationary binary distribution, namely those that include the highest and lowest probable states reached, are those satisfying:

$$-\rho(x) + \frac{-x}{ab(1-\varepsilon)} + \frac{a-1}{a(1-\varepsilon)} = 0, \quad (16)$$

where $\rho(x)$ is defined in (3). On the other hand, making zero the right hand side of equation

(4) and re-ordering terms, the set of all possible equilibria satisfies:

$$-\rho(x) + \frac{-x}{ab(1-\varepsilon)} + \frac{1}{(1-\varepsilon)} = 0, \quad (17)$$

Both expressions (16) and (17) are quite similar differing only in their respective last term of the left hand side, which get closer as $a \rightarrow \infty$, what implies large transcription rate as compared with protein degradation. This means that the most probable states of the microscopic system are near the stable equilibrium points described by the deterministic counterpart. Moreover, they become closer as parameter a increases.

In Fig. 8 the smallest eigenvalue is depicted in absolute value. In the second row of this figure we represent $\ln(-\lambda_1)$ to appreciate clearly how the eigenvalue evolves with parameters a , b . The logarithm of the eigenvalue decreases as the parameters a and b become higher and smaller, respectively. Variations of the logarithm of the eigenvalue are more pronounced inside the bimodal and bistable regions. Moreover, as discussed in [26] as the parameter a increases the system approaches the deterministic limit. This explains why hysteresis can be mistaken due to the very slow dynamics of the stochastic system for gene networks with high a and small b parameters.

Fig. 9 compares the set of stable and unstable equilibrium states obtained from a deterministic representation (blue lines) with the most and least probable microscopic states (black lines) respectively. Note that this equivalence does not support the existence of hysteresis at the microscopic level. Essentially, what the picture shows is that, rather than a parameter-dependent preferential state among two stable ones, there are two highly probable states that coexist for a given parameter region on a cell population.

Invoking pseudo-potential concepts to interpret dynamics in GRN under fluctuations (e.g. [12]), although attractive from an intuitive point of view, may be misleading since it cannot capture the notion of coexistence. The pseudo-potential land is not easy to compute either, specially when increasing the dimension of the space of proteins. On the other hand the negative of the solution of (5), namely $-p(\tau, x)$, seems the natural landscape capturing the evolution of the underlying microscopic system. It has a quite amenable form for computation not just in simple one dimensional cases as the one studied but also in larger dimensional protein spaces.

4 List of Figures

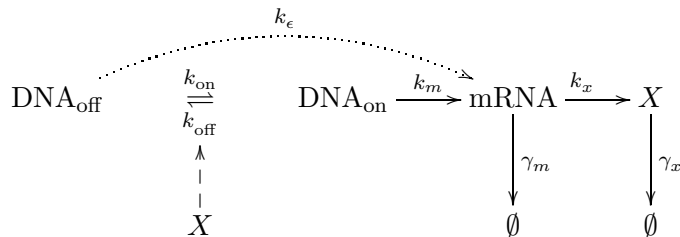


Figure 1: Self-regulatory transcription-translation mechanism. The promoter is assumed to switch between active (DNA_{on}) and inactive (DNA_{off}) states, with rate constants k_{on} and k_{off} per unit time, respectively. The transition is assumed to be controlled by a feedback mechanism induced by the binding/unbinding of a given number of X -protein molecules. Transcription of messenger RNA (mRNA) from the active DNA form, and translation into protein X are assumed to occur at rates (per unit time) k_m and k_x , respectively. k_ϵ is the rate constant associated with transcriptional leakage. The mRNA and protein degradations are assumed to occur by first order processes with rate constants γ_m and γ_x , respectively.

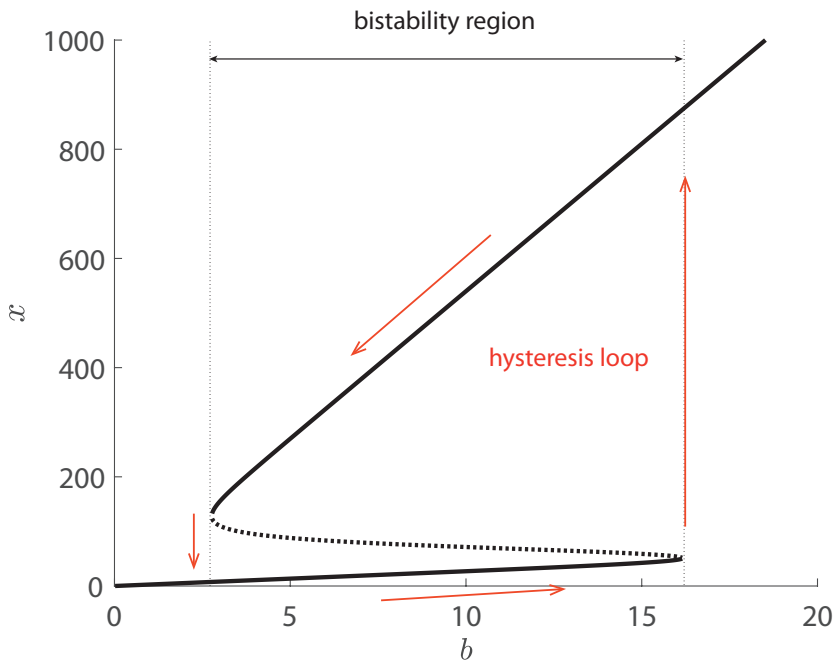


Figure 2: Steady-state solutions of the deterministic system (4) as a function of parameter b ($a = 54$). The parameters of the Hill function employed along the paper are $H = -7$ and $K = 100$. The plot shows two saddle-node bifurcations [27] with a parameter region leading to three equilibrium states. For each parameter value, there is one unstable state (in dotted line), bounded by two stable ones (in continuous lines).

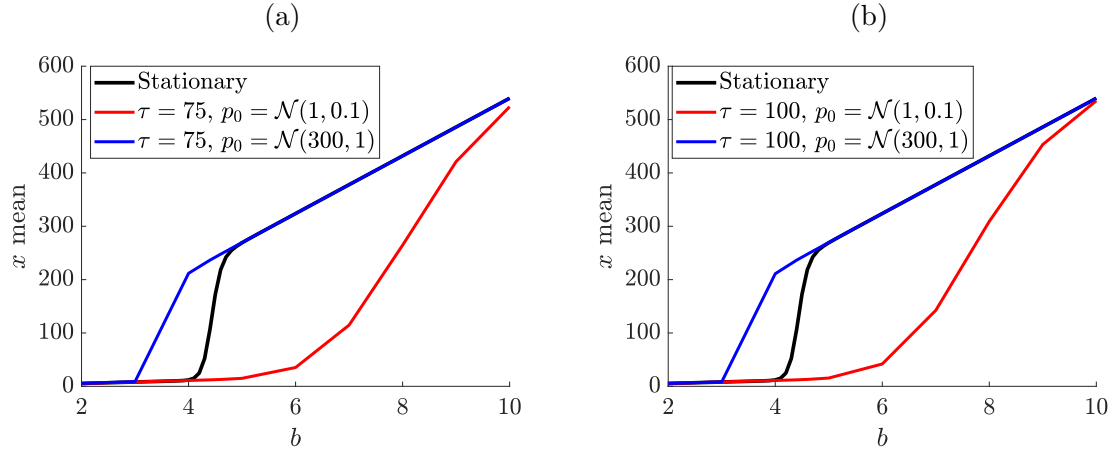


Figure 3: Mean x -values plotted as a function of parameter b ($a = 54$). The black line corresponds to the stationary solution of the PIDE model (5). Red and blue lines are transient solutions from initial conditions $p(0, x) = \mathcal{N}(1, 0.1)$ and $p(0, x) = \mathcal{N}(300, 1)$, respectively at $\tau = 75$ (a) and $\tau = 100$ (b). $\mathcal{N}(\mu, \sigma)$ is the Gaussian distribution with mean μ and standard deviation σ . Slow transients lead to multiple mean states that can be confounded with hysteresis. This is in conflict with the corresponding stationary solution associated to the master equation which is unique and therefore can only lead to one mean x -value per b value.

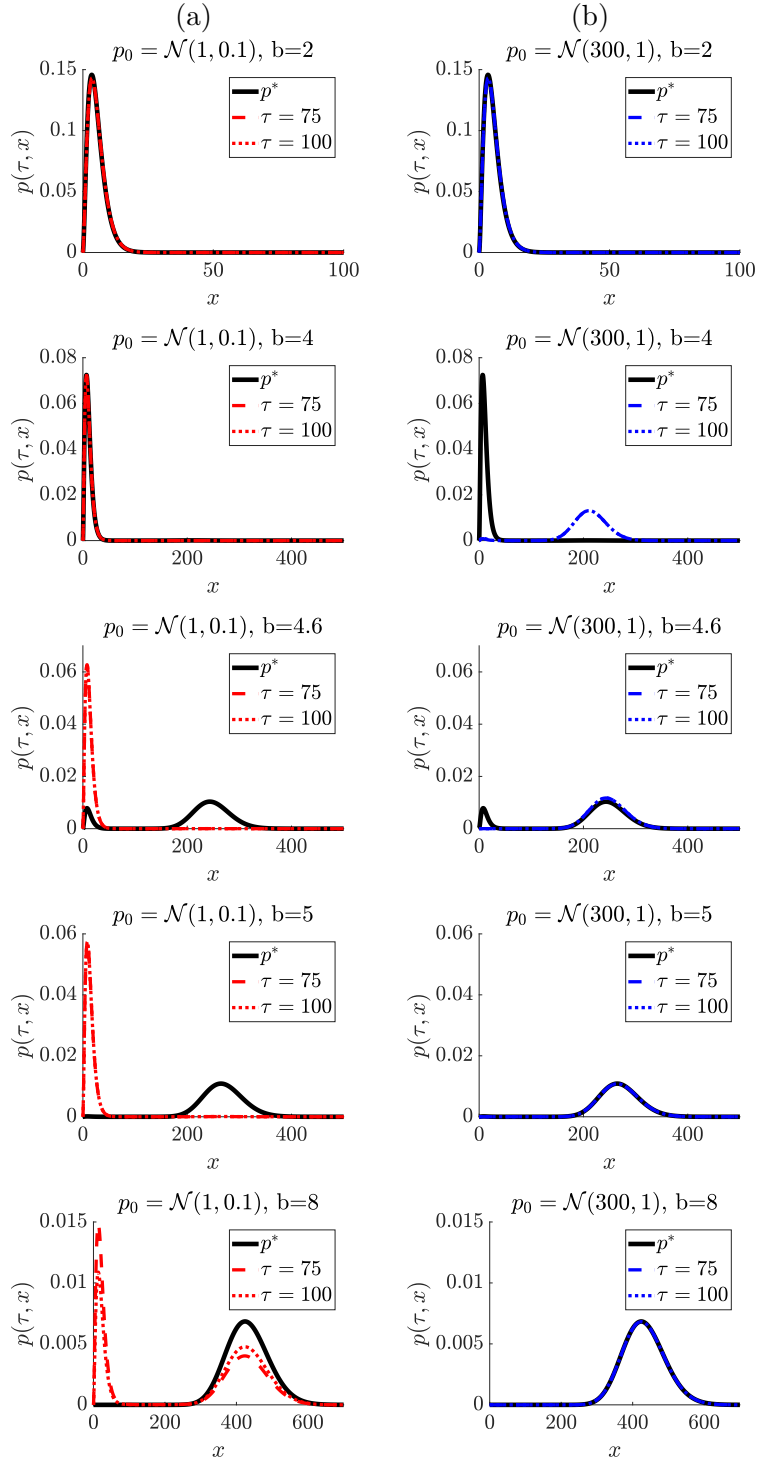


Figure 4: Stationary and transient distributions obtained for different values of the b parameter ($a = 54$). Transient distributions are represented by dashed ($\tau = 75$) and dotted ($\tau = 100$) lines. The black line is the stationary distribution. The initial conditions are (a) $p(0, x) = \mathcal{N}(1, 0.1)$ and (b) $p(0, x) = \mathcal{N}(300, 1)$.

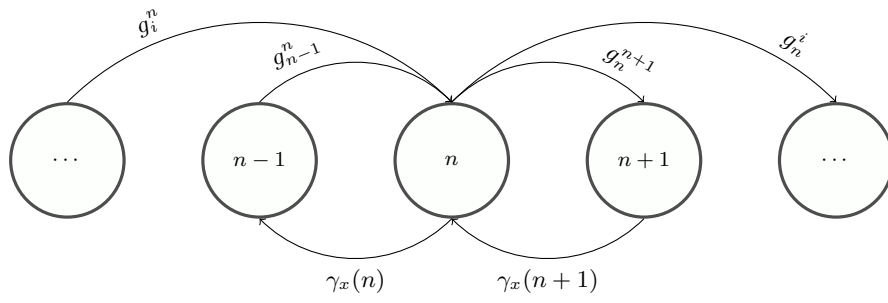


Figure 5: Jump process representation of one protein produced in bursts, where one state n can be reached from lower states $0 \leq i < n$ with different transition probability functions g_i^n . Equivalently, from the state n the protein number can jump to higher states i with transition probability function g_n^i . The degradation follows a one step process (i. e. from state n to state $n - 1$).

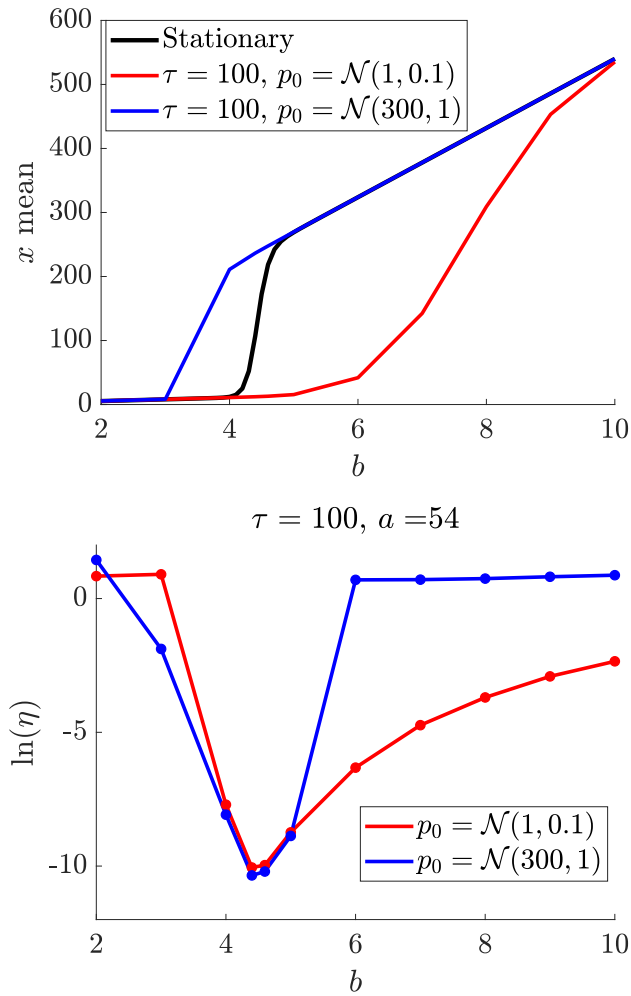


Figure 6: For the set of transient and equilibrium mean x -values plotted as a function of parameter b (upper plot), the lower plot shows the corresponding convergence rates of the solution towards the equilibrium distribution in logarithmic scale for two different initial conditions. The parameter region leading to bimodal distributions corresponds with the slowest convergence rates. Such slow dynamics might be experimentally mistaken with stationary solutions what would be misinterpreted as showing hysteresis behaviour. If the system is allowed to achieve the equilibrium, hysteresis disappears.

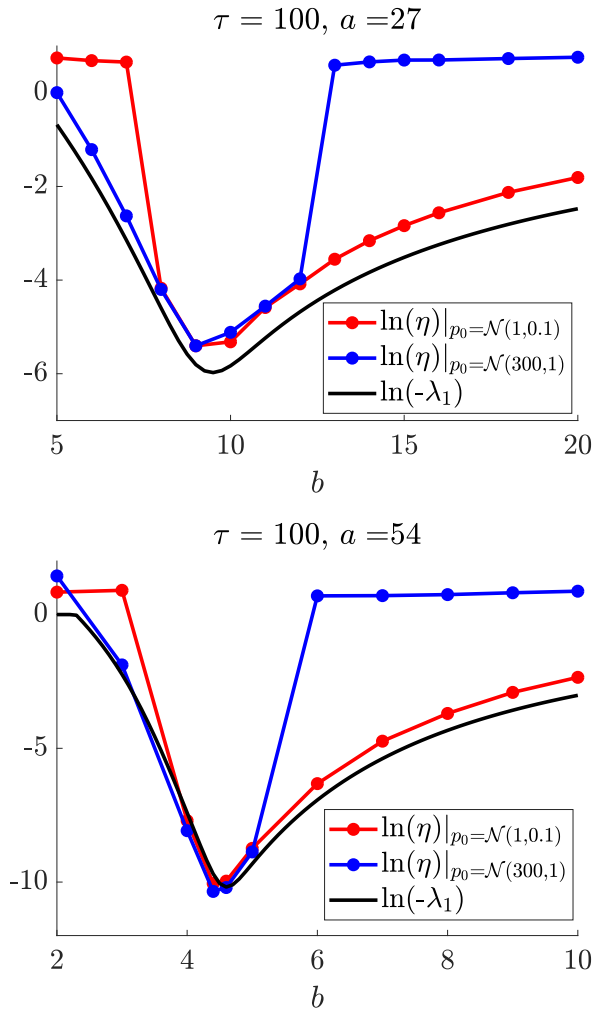


Figure 7: Comparison of the logarithms of the ratios of convergence η and the highest eigenvalues of the matrix \mathcal{M} of the discrete version of the PIDE model, at $\tau = 100$, from two initial conditions in the form of Dirac deltas.

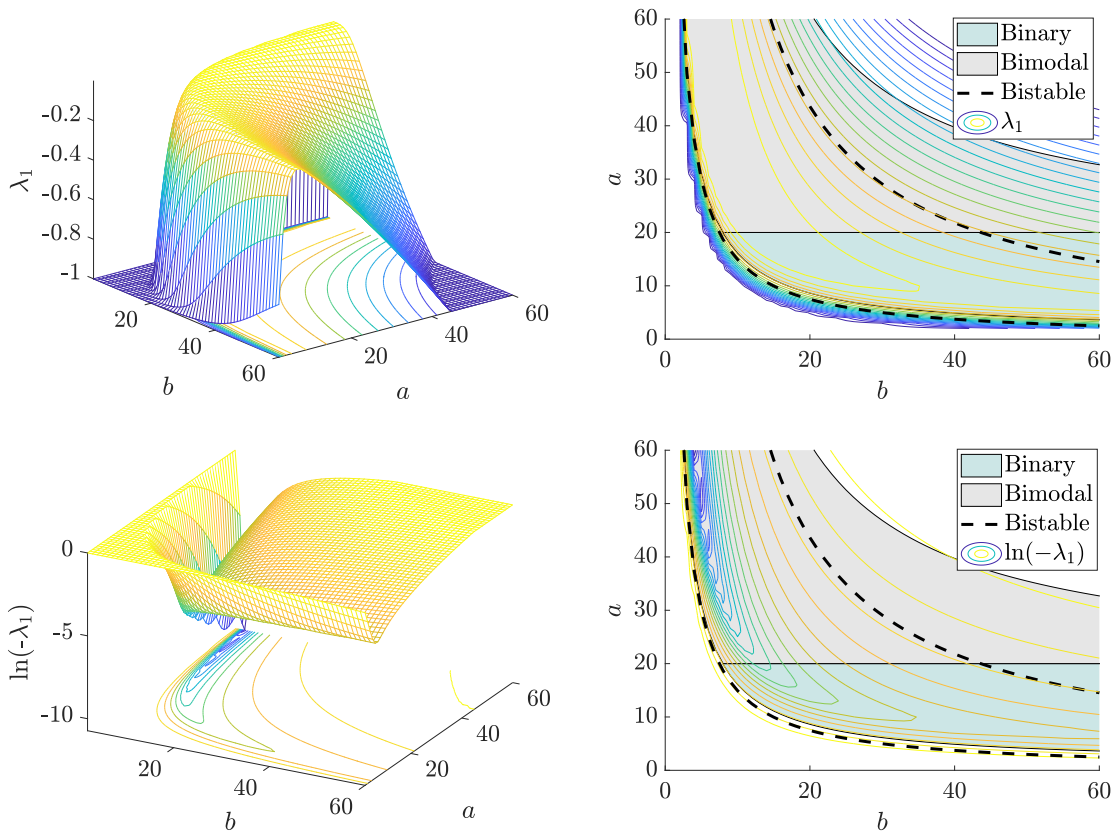


Figure 8: First row shows the eigenvalue λ_1 while second row represents a logarithmic scale of λ_1 , $\ln(-\lambda_1)$, in the parameter space a and b . Second column depicts a contour of the plots at the first column over the regions where distributions have two peaks in the stochastic representation (binary and bimodal) and the region where the deterministic system is bistable, which have been computed by the algorithm in [18].

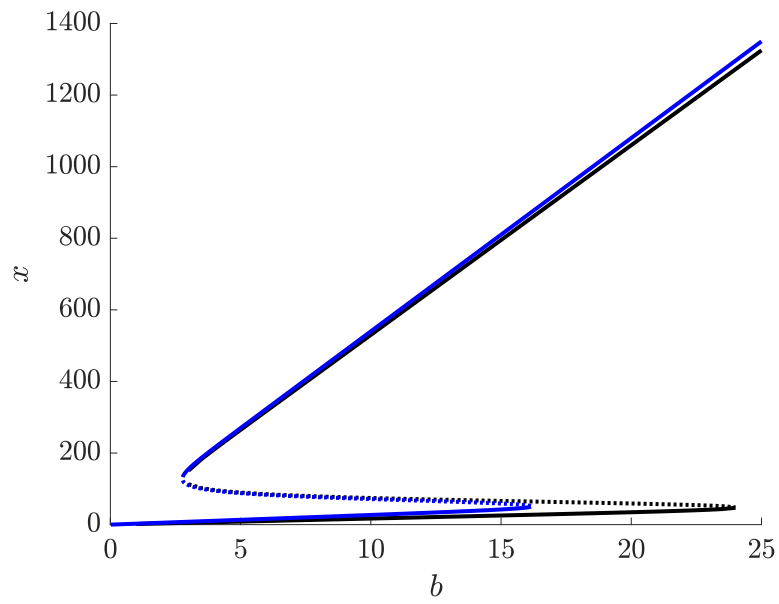


Figure 9: Equilibrium states obtained from a deterministic representation (blue lines) as compared with the extremes (maxima and minimum) of the distributions that result from a stochastic description (black lines). Blue dotted lines correspond with unstable steady states whereas black dotted lines identify the minimum of the bimodal distribution.

References

- [1] J. Veening, WK Smits, , and O. Kuipers. Bistability, epigenetics and bet-hedging in bacteria. *Annu. Rev. Microbiol.*, 62:193–210, 2008.
- [2] R. Losick and C. Desplan. Stochastic state transitions give rise to phenotypic equilibrium in populations of cancer cells. *Science*, 320(5872):65–68, 2008.
- [3] N. G. Van Kampen. *Stochastic Processes in Physics and Chemistry*. Elsevier, Netherlands, third edition, 2007.
- [4] E.M. Ozbudak, M. Thattai, H.N. Lim, B.I. Shraiman, and A. van Oudenaarden. Multistability in the lactose utilization network of *Escherichia coli*. *Nature*, 427:737–740, 2008.
- [5] P. Thomas, N. Popovic, and R Grima. Phenotypic switching in gene regulatory networks. *Proceedings of the National Academy of Sciences USA*, 111(19):6994–6999, 2014.
- [6] R. Gnügge, L. Dharmarajan, M. Lang, and J. Stelling. An Orthogonal Permease–Inducer–Repressor Feedback Loop Shows Bistability. *ACS Synth. Biol.*, 5:1098–1107, 2016.
- [7] C. Hsu, V. Jaquet, M. Gencoglu, and A. Becskei. Protein Dimerization Generates Bistability in Positive Feedback Loops. *Cell Reports*, 16(5):1204–1210, 2016.
- [8] W. Xiong and J.E. Ferrell. A positive-feedback-based bistable memory module that governs a cell fate decision. *Nature*, 426:460–465, 2012.
- [9] L. Wang, B.L. Walker, S. Iannaccone, D. Bhatt, P. J. Kennedy, and W. T. Tse. Bistable switches control memory and plasticity in cellular differentiation. *Proc. Natl. Acad. Sci. U.S.A.*, 106(16):6638–6643, 2009.
- [10] J.E. Ferrell. Bistability, bifurcations, and waddington’s epigenetic landscape. *Nature*, 22(11):R458–R466, 2012.
- [11] P.B. Gupta, C.M Fillmore, G. Jiang, Shapira S.D., K. Tao, C. Kuperwasser, and Lander E.S. Stochastic state transitions give rise to phenotypic equilibrium in populations of cancer cells. *Cell*, 146(4):633–644, 2011.
- [12] M. Wu, R.Q. Su, X. Li, T. Ellis, Y.G. Lai, and X. Wang. Engineering of regulated stochastic cell fate determination. *Proc. Natl. Acad. Sci. U.S.A.*, 110(26):10610–10615, 2013.
- [13] X. Fang, Q. Liu, C. Bohrer, Z. Hensel, W. Han, J. Wang, and J. Xiao. Cell fate potentials and switching kinetics uncovered in a classic bistable genetic switch. *Nature Communications*, 9:2787, 2018.
- [14] J. Wang. Landscape and flux theory of non-equilibrium dynamical systems with application to biology. *Advances in Physics*, 64(1):1–137, 2015.

- [15] M. Pájaro, A. A. Alonso, I. Otero-Muras, and C. Vázquez. Stochastic modeling and numerical simulation of gene regulatory networks with protein bursting. *J. Theor. Biol.*, 421:51–70, 2017.
- [16] M. Pájaro, I. Otero-Muras, C. Vázquez, and A. A. Alonso. SELANSI: a toolbox for Simulation of Stochastic Gene Regulatory Networks. *Bioinformatics*, 34(5):893–895, 2018.
- [17] A. Ochab-Marcinek and M. Tabaka. Transcriptional leakage versus noise: A simple mechanism of conversion between binary and graded response in autoregulated genes. *Phys. Rev. E*, 91(1):012704, 2015.
- [18] M. Pájaro, A. A. Alonso, and C. Vázquez. Shaping protein distributions in stochastic self-regulated gene expression networks. *Phys. Rev. E*, 92(3):032712, 2015.
- [19] U. Alon. *An Introduction to Systems Biology. Design Principles of Biological Circuits*. Chapman & Hall/ CRC, London, 2007.
- [20] R. D. Dar, B. S. Razooky, A. Singh, T. V. Trimeloni, J. M. McCollum, C. D. Cox, M. L. Simpson, and L. S. Weinberger. Transcriptional burst frequency and burst size are equally modulated across the human genome. *Proc. Natl. Acad. Sci. U.S.A.*, 109(43):17454–17459, 2012.
- [21] E. M. Ozbudak, M. Thattai, I. Kurtser, A. D. Grossman, and A. van Oudenaarden. Regulation of noise in the expression of a single gene. *Nature Genet.*, 31(1):69–73, 2002.
- [22] N. Friedman, L. Cai, and X. S. Xie. Linking stochastic dynamics to population distribution: An analytical framework of gene expression. *Phys. Rev. Lett.*, 97(16):168302, 2006.
- [23] J. A. Cañizo, J. A. Carrillo, and M. Pájaro. Exponential equilibration of genetic circuits using entropy methods. *J. Math. Biol.*, <https://doi.org/10.1007/s00285-018-1277-z>, 2018.
- [24] M. Pájaro, A. A. Alonso, J. A. Carrillo, and C. Vázquez. Stability of stochastic gene regulatory networks using entropy methods. *IFAC-PapersOnLine*, 49(24):1–5, 2016.
- [25] D. Fife. Which linear compartmental systems contain traps? *Math. Biosci.*, 14(3-4):311–315, 1972.
- [26] M. Pájaro and A. A. Alonso. On the applicability of deterministic approximations to model genetic circuits. *IFAC-PapersOnLine*, 49(7):206–211, 2016.
- [27] R. Seydel. *Practical bifurcation and stability analysis*. Springer, New York, 2010.